Statistics-based Bayesian Modeling Framework for Uncertainty Quantification and Propagation

Menghao Ping [a,b], Xinyu Jia [b], Costas Papadimitriou [b,*], Xu Han [a], Chao Jiang [a]

[a] State Key Laboratory of Advanced Design and Manufacturing for Vehicle Body, College of Mechanical and Vehicle Engineering, Hunan University, Changsha, China
[b] Department of Mechanical Engineering, University of Thessaly, Volos, Greece

Abstract

A new Bayesian modeling framework is proposed to account for the uncertainty in the model parameters arising from model and measurements errors, as well as experimental, operational, environmental and manufacturing variabilities. Uncertainty is embedded in the model parameters using a single level hierarchy where the uncertainties are quantified by Normal distributions with the mean and the covariance treated as hyperparameters. Unlike existing hierarchical Bayesian modelling frameworks, the likelihood function for each observed quantity is built based on the Kullback–Leibler divergence used to quantify the discrepancy between the probability density functions (PDFs) of the model predictions and measurements. The likelihood function is constructed assuming that this discrepancy for each measured quantity follows a truncated normal distribution. For Gaussian PDFs of measurements and response predictions, the posterior PDF of the model parameters depends on the lower two moments of the respective PDFs. This representation of the posterior is also used for non-Gaussian PDFs of measurements and model predictions to approximate the uncertainty in the model parameters. The proposed framework can tackle the situation where only PDFs or statistical characteristics are available for measurements. The propagation of uncertainties is accomplished through sampling. Two applications demonstrate the use and effectiveness of the proposed framework. In the first one, structural model parameter inference is considered using simulated statistics for the modal frequencies and mode shapes. In the second one, uncertainties in the parameters of the probabilistic *S-N* curves used in fatigue are quantified based on experimental data.

Keywords: Bayesian inference; Kullback-Leibler divergence; Uncertainty quantification and propagation; Structural dynamics; Fatigue

1. Introduction

The general Bayesian statistical framework proposed by Beck and Katafygiotis [1] provides a rigorous mathematical means to address the model updating problem under uncertainty. Based on this framework, there have been a lot of works for various applications, such as parameter estimation [2-7], model selection [8,9], damage identification [10-12], and robust uncertainty propagation [13,14], among which the parameter estimation application serving as the foundation of other applications has kept the overwhelming attention. The Bayesian parameter inference is accomplished by embedding a parameterized probabilistic model to describe the discrepancy between model predictions and measurements. Then the formulation for the posterior distribution of the structural and prediction error model parameters is provided as a product of the likelihood function and the prior distribution of the model parameters. To estimate the posterior distribution of the model parameters, the likelihood function is usually built based on a relation function between model predictions and measurements by defining a probabilistic structure of the prediction error.

For industrial applications, the parameter estimation results from different measurements show distinct variations. The variation usually arises from load uncertainty, model error,

measurement noise, and changing environmental/operational conditions [15-17]. Variations in the parameters of a model introduced to simulate a population of identically manufactured structures are also obtained due to manufacturing variabilities [18, 19]. Therefore, it is important to describe these variations. The hierarchical Bayesian modeling framework (HBM) [20-26] has been proposed to quantify the uncertainty in the model parameters and prediction errors due to the aforementioned variabilities. The core of HBM is using a parameterized prior distribution of model parameters by introducing an extra layer involving hyper parameters to describe the variation of model parameters.

In this paper, a new probabilistic model is proposed on the basis of Bayesian framework, and the main difference is the principle to build the likelihood function, which is based on the relationship of statistics between model predictions and measurements for each model output. Compared with HBM, it does not require collecting datasets, and measurements can be the PDFs or statistics of measured quantities, so its application is more universal. It can also handle cases for which only the statistics like mean and variance are available from the measurements. In such cases it is unreasonable to build datasets in terms of samples generated from them and then apply existing conventional or hierarchical Bayesian modeling frameworks.

This paper is organized as follow. In Section 2, the new proposed Bayesian modeling framework is described in detail, including construction of the proposed probabilistic model, uncertainty quantification of parameters, and uncertainty propagation to quantities of interest (QoI). The application to structural dynamics based on measured modal properties is presented in Section 3. In Section 4, a three-DOF spring mass chain system is taken as a simulated example to illustrate the effectiveness of the proposed framework. The application to the parameter inference and uncertainty quantification of probabilistic *S-N* curves used in fatigue damage accumulation is given in Section 5. Conclusions are presented in Section 6.

2. Proposed Bayesian Modeling Framework

2.1 Probabilistic model

Figure 1 shows the structure of the proposed probabilistic modeling framework. Assume a parameterized model of a structural system and let $q_k(\boldsymbol{\theta})$, $k=1,\cdots,n_q$ be the model predictions for n_q output quantities, where $\boldsymbol{\theta}$ is model parameter vector to be identified by measurements available for these output quantities. To account for model error and environmental/operational variabilities in the model predictions, an additive error term e_k is considered so that the predictions from the model are taken as

$$\tilde{q}_k(\boldsymbol{\theta}) = q_k(\boldsymbol{\theta}) + w_k e_k \tag{1}$$

where w_k is a weighting factor that scales the error terms e_k.

Uncertainties are embedded in the model parameter set $\boldsymbol{\theta}$ by assigning to the set $\boldsymbol{\theta}$ a Gaussian distribution with mean vector $\boldsymbol{\mu}_{\boldsymbol{\theta}}$ and covariance matrix $\boldsymbol{\Sigma}_{\boldsymbol{\theta}}$. To account for the unmodelled dynamics, the error term e_k is assumed to follow a Gaussian distribution $\mathrm{N}\left(e_k \mid 0, \sigma_e^2\right)$ with zero mean and variance σ_e^2, where the general notation $\mathrm{N}(\mathbf{x} \mid \boldsymbol{\mu}, \boldsymbol{\Sigma})$ is introduced to denote a multivariable normal distribution evaluated at $\mathbf{x}$ with mean vector $\boldsymbol{\mu}$ and covariance matrix $\boldsymbol{\Sigma}$. It should be noted that the weights w_k introduced in Eq. (1) provides the flexibility to scale differently the error term e_k for each quantity of interest $\tilde{q}_k(\boldsymbol{\theta})$. This is needed when the intensities of the measured or response quantities involved in Eq. (1) have considerable differences for each k. In this case it is best to choose w_k values

to correspond to a measure of the intensity of the respective measured or response quantity, such as the mean of the measured or response quantity.

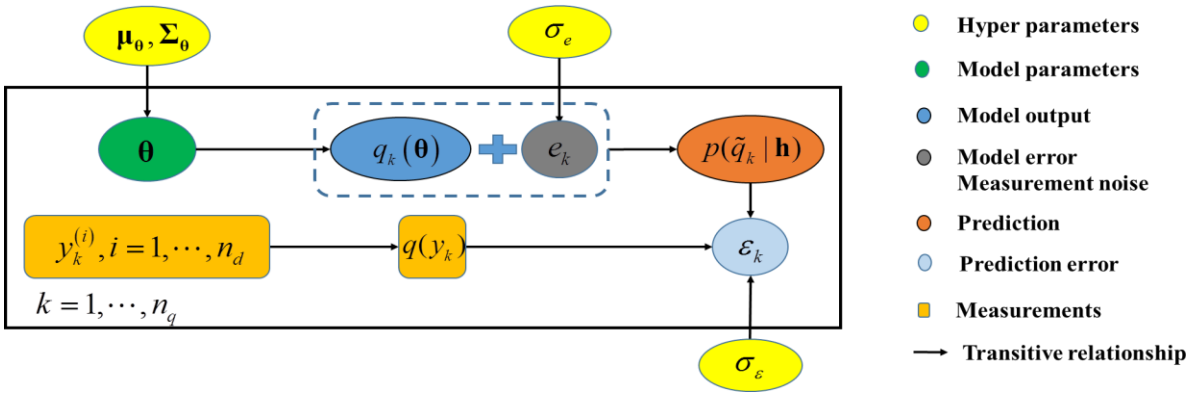

Figure 1 Proposed probabilistic modeling framework

To distinguish from the model parameters $\boldsymbol{\theta}$ and the error term e_k, the parameters $\mathbf{h} = \{\boldsymbol{\mu}_{\boldsymbol{\theta}}, \boldsymbol{\Sigma}_{\boldsymbol{\theta}}, \sigma_e\}$ are called hyper parameters. Given the hyper parameters, one can obtain the conditional PDF $p(\tilde{q}_k \mid \mathbf{h})$ of k-th model output quantity $\tilde{q}_k$ given the values of the hyper parameters $\mathbf{h}$ by propagating the uncertainties in the model parameters $\boldsymbol{\theta}$ and the error term e_k.

For a conditional PDF that can be approximated by a Gaussian distribution, one has $p(\tilde{q}_k \mid \mathbf{h}) = \mathrm{N}(\tilde{q}_k \mid \mu_{\tilde{q}_k|\mathbf{h}}, \sigma^2_{\tilde{q}_k|\mathbf{h}})$, where $\mu_{\tilde{q}_k|\mathbf{h}}$ is the mean and $\sigma^2_{\tilde{q}_k|\mathbf{h}}$ is the variance of $\tilde{q}_k$ given $\mathbf{h}$. In particular, a Gaussian distribution arises for the case of a linear model $\mathbf{q}(\boldsymbol{\theta}) = \mathbf{A}\boldsymbol{\theta} + \mathbf{b}$, where $\mathbf{q} = \left[q_1, \ldots, q_{n_q}\right]^{\mathrm{T}}$, $\mathbf{A} = [\mathbf{a}_1^T, \ldots, \mathbf{a}_{n_q}^T]^{\mathrm{T}}$, $\mathbf{b} = [b_1, \ldots, b_{n_q}]^{\mathrm{T}}$ and $\mathbf{a}_k$, $k = 1, \ldots, n_q$, is the k-th row (vector) of $\mathbf{A}$ with the same dimension as $\boldsymbol{\theta}$. Given $\boldsymbol{\mu}_{\boldsymbol{\theta}}$, $\boldsymbol{\Sigma}_{\boldsymbol{\theta}}$ and σ_e, one readily derives that the mean $\mu_{\tilde{q}_k|\mathbf{h}}$ and the variance $\sigma^2_{\tilde{q}_k|\mathbf{h}}$ of the quantity $\tilde{q}_k$ in terms of the hyperparameters $\mathbf{h}$ as follows

$$\mu_{\tilde{q}_k|\mathbf{h}} = \mathbf{a}_k \boldsymbol{\mu}_{\boldsymbol{\theta}} + b_k \tag{2}$$

$$\sigma^2_{\tilde{q}_k|\mathbf{h}} = \mathbf{a}_k \boldsymbol{\Sigma}_{\boldsymbol{\theta}} \mathbf{a}_k^{\mathrm{T}} + w_k^2 \sigma_e^2 \tag{3}$$

The PDF of k-th model output $P_{\tilde{q}_k|\mathbf{h}}$ can be directly obtained in the form

$$p(\tilde{q}_k \mid \mathbf{h}) = \mathrm{N}(\tilde{q}_k \mid \mu_{\tilde{q}_k|\mathbf{h}}, \sigma^2_{\tilde{q}_k|\mathbf{h}}) = \mathrm{N}(\tilde{q}_k \mid \mathbf{a}_k \boldsymbol{\mu}_{\boldsymbol{\theta}} + b_k, \mathbf{a}_k \boldsymbol{\Sigma}_{\boldsymbol{\theta}} \mathbf{a}_k^{\mathrm{T}} + w_k^2 \sigma_e^2) \tag{4}$$

For nonlinear models, the PDF $p(\tilde{q}_k \mid \mathbf{h}) = p(\tilde{q}_k \mid \boldsymbol{\mu}_{\boldsymbol{\theta}}, \boldsymbol{\Sigma}_{\boldsymbol{\theta}}, \sigma_e)$ of k-th model output can be derived by the total probability theorem as

$$\begin{aligned} p\left(\tilde{q}_k \mid \boldsymbol{\mu}_{\boldsymbol{\theta}}, \boldsymbol{\Sigma}_{\boldsymbol{\theta}}, \sigma_e\right) &= \int_{\boldsymbol{\theta}} p\left(\tilde{q}_k \mid \boldsymbol{\theta}, \sigma_e\right) \mathrm{N}\left(\boldsymbol{\theta} \mid \boldsymbol{\mu}_{\boldsymbol{\theta}}, \boldsymbol{\Sigma}_{\boldsymbol{\theta}}\right) d\boldsymbol{\theta} \\ &\approx \frac{1}{n_s} \sum_{j}^{n_s} \mathrm{N}\left(\tilde{q}_k \mid q_k\left(\boldsymbol{\theta}^{(j)}\right), w_k^{2(j)} \sigma_e^2\right) \end{aligned} \tag{5}$$

where $\boldsymbol{\theta}^{(j)}$, $j = 1, \ldots, n_s$, are sampled from $\mathrm{N}\left(\boldsymbol{\theta} \mid \boldsymbol{\mu}_{\boldsymbol{\theta}}, \boldsymbol{\Sigma}_{\boldsymbol{\theta}}\right)$. The structure of the model error in Eq. (1) was used to replace conditional PDF $p\left(\tilde{q}_k \mid \boldsymbol{\theta}, \sigma_e\right)$ in Eq. (5) by a normal PDF $\mathrm{N}\left(\tilde{q}_k \mid q_k\left(\boldsymbol{\theta}\right), w_k^2 \sigma_e^2\right)$ with mean $q_k\left(\boldsymbol{\theta}\right)$ and variance $w_k^2 \sigma_e^2$.

Let $\pi(y_k)$ denotes the PDF of *k*-th measured quantity y_k, so that the PDFs for all the measurements are $\{\pi(y_k),\ k=1,\cdots,n_q\}$. For the situation where the measurements are the statistics of measured quantities, the $\pi(y_k)$ can be directly obtained by moments-based PDF simulation methods, like maximum entropy method (MEM) [27,28]. For the situation where only measured data $D_k=\{y_k^{(i)}, i=1,\cdots,n_d\}$ are available for the *k*-th measured quantity y_k, where n_d denotes the number of measured data of *k*-th measured quantity, the kernel density estimation (KDE) [29,30] can be used to simulate $\pi(y_k)$ for sufficient large number of measurements n_d, as follows

$$\pi(y_k)=\frac{1}{n_d\times h}\sum_i^{n_d}K\left(\frac{y_k-y_k^{(i)}}{h}\right) \tag{6}$$

Also, if n_d is not big enough, $\pi(y_k)$ can be assumed to be a Gaussian distribution with mean and variance calculated by the data set D_k.

Given $\pi(y_k)$ and $p(\tilde{q}_k\,|\,\mathbf{h})$, the discrepancy between them is then quantified by the Kullback–Leibler divergence (KL-div) [31]. However, considering the asymmetry of KL-div, a symmetric measure of the discrepancy can be used, defined as

$$\begin{aligned}\varepsilon_k(y_k,\tilde{q}_k\,|\,\mathbf{h}) &= D_{KL}\left[\pi,p\right]+D_{KL}\left[p,\pi\right]\\ &=\frac{1}{2}\int_x\pi(x)\log\left(\frac{\pi(x)}{p(x\,|\,\mathbf{h})}\right)dx+\frac{1}{2}\int_x p(x\,|\,\mathbf{h})\log\left(\frac{p(x\,|\,\mathbf{h})}{\pi(x)}\right)dx\end{aligned} \tag{7}$$

For a Gaussian distribution $p(\tilde{q}_k\,|\,\mathbf{h})=\mathrm{N}(\tilde{q}_k\,|\,\mu_{\tilde{q}_k|\mathbf{h}},\sigma^2_{\tilde{q}_k|\mathbf{h}})$ of $\tilde{q}_k$ given $\mathbf{h}$ and for *k*-th measurement that is Gaussian distributed, i.e. $\pi(y_k)=\mathrm{N}(y_k\,|\,\mu_{y_k},\sigma^2_{y_k})$ for all *k*, the KL-div simplifies to the analytical form

$$\begin{aligned}\varepsilon_k(y_k,\tilde{q}_k\,|\,\mathbf{h}) &= \frac{1}{4}\left\{\log\left[\frac{\sigma^2_{\tilde{q}_k|\mathbf{h}}}{\sigma^2_{y_k}}\right]+\frac{\sigma^2_{y_k}}{\sigma^2_{\tilde{q}_k|\mathbf{h}}}+\frac{\left[\mu_{y_k}-\mu_{\tilde{q}_k|\mathbf{h}}\right]^2}{\sigma^2_{\tilde{q}_k|\mathbf{h}}}-1\right\}\\ &\quad+\frac{1}{4}\left\{\log\left[\frac{\sigma^2_{y_k}}{\sigma^2_{\tilde{q}_k|\mathbf{h}}}\right]+\frac{\sigma^2_{\tilde{q}_k|\mathbf{h}}}{\sigma^2_{y_k}}+\frac{\left[\mu_{y_k}-\mu_{\tilde{q}_k|\mathbf{h}}\right]^2}{\sigma^2_{y_k}}-1\right\}\\ &=\frac{1}{4}\left[\frac{\sigma^2_{\tilde{q}_k|\mathbf{h}}}{\sigma^2_{y_k}}-1\right]+\frac{1}{4}\left[\frac{\sigma^2_{y_k}}{\sigma^2_{\tilde{q}_k|\mathbf{h}}}-1\right]+\frac{1}{4}\frac{\left[\mu_{y_k}-\mu_{\tilde{q}_k|\mathbf{h}}\right]^2}{\sigma^2_{\tilde{q}_k|\mathbf{h}}}\left[1+\frac{\sigma^2_{\tilde{q}_k|\mathbf{h}}}{\sigma^2_{y_k}}\right]\end{aligned} \tag{8}$$

Note that the first two terms give a measure of the error between the variance of the experimental value and the variance predicted from the model. These two terms become zero when the variance $\sigma^2_{y_k}$ of the experimental value equals the variance $\sigma^2_{\tilde{q}_k|\mathbf{h}}$ of the model prediction. Also, the last term gives the error between the mean of the experimental value and the mean of the model predictions. When the mean of the experimental value is equal to the mean of the model predictions, then the third term disappears. The discrepancy as defined by KL-div is a weighted sum of the discrepancies between the variances of the two PDFs and the means of the two PDFs. However, the KL-div measure is a rational method to assign the weights which otherwise one would have to select arbitrarily.

For non-Gaussian PDFs arising from nonlinear models, Eq. (8) for the KL-div can also be used as an approximate measure of the discrepancy between the two PDFs in terms of the

first two moments of the PDFs. Alternatively, for nonlinear models, the integral can be approximated by Monte Carlo (MC) sample estimates

$$\varepsilon_k(y_k,\tilde{q}_k\,|\,\mathbf{h}) \approx \frac{1}{2n}\sum_i^n \log\left(\frac{\pi\left(y_k^{(i)}\right)}{p\left(y_k^{(i)}\,|\,\mathbf{h}\right)}\right)+\frac{1}{2n}\sum_i^n \log\left(\frac{p\left(\tilde{q}_k^{(i)}\right)}{\pi\left(\tilde{q}_k^{(i)}\right)}\right) \tag{9}$$

where $y_k^{(i)}$ and $\tilde{q}_k^{(i)}$, $i=1,\cdots,n$, are the samples distributed as $\pi(y_k)$ and $p(\tilde{q}_k\,|\,\mathbf{h})$, respectively. Estimating the KL-div from Eq. (9) requires a large number of samples and can be a computationally very tedious procedure. Simplified approximations, such as Eq. (8), based on the first two moments of the non-Gaussian PDFs are preferred.

2.2 Estimation of hyper parameters uncertainty

The first task of uncertainty quantification is to identify the hyper parameters in the proposed probabilistic model. This is accomplished by introducing a probabilistic model to represent the variables $\varepsilon=\left\{\varepsilon_k, k=1,\cdots,n_q\right\}$ quantifying the discrepancy between the PDF of the model predictions and the measurements. Specifically, the variables in the set $\varepsilon=\left\{\varepsilon_k, k=1,\cdots,n_q\right\}$ are assumed to follow a truncated normal distribution $\mathrm{TN}\left(\varepsilon_k\,|\,0,{\sigma_\varepsilon}^2\right), \varepsilon_k\geq 0$ because of the non-negative values of KL-div, with the parameter σ_ε be another hyper parameter to be inferred from the data. Thus, in the proposed probabilistic model, the hyper parameters can be categorized into two types: one is to describe the uncertainty of the prediction model, which comprises $\mathbf{h}=\{\boldsymbol{\mu}_\mathbf{0},\boldsymbol{\Sigma}_\mathbf{0},\sigma_e\}$ and the other is σ_ε.

According to the relationship between measurements and model predictions described by Eq. (7), the Bayes theorem is applied to infer the posterior distribution of hyper parameters as

$$p\left(\mathbf{h},\sigma_\varepsilon\,|\,\varepsilon\right)\propto p\left(\varepsilon\,|\,\mathbf{h},\sigma_\varepsilon\right)p\left(\mathbf{h}\right)p\left(\sigma_\varepsilon\right) \tag{10}$$

where $p\left(\mathbf{h},\sigma_\varepsilon\,|\,\varepsilon\right)$ is joint posterior distribution; $p\left(\mathbf{h}\right)$ and $p\left(\sigma_\varepsilon\right)$ are the prior distributions assuming that $\mathbf{h}$ and σ_ε are independent; and $p\left(\varepsilon\,|\,\mathbf{h},\sigma_\varepsilon\right)$ is the likelihood function. Assuming that ε_k in $\varepsilon=\left\{\varepsilon_k, k=1,\cdots,n_q\right\}$ are independent, the likelihood function takes the form

$$p\left(\varepsilon\,|\,\mathbf{h},\sigma_\varepsilon\right)=\prod_{k=1}^{n_q} p\left(\varepsilon_k\,|\,\mathbf{h},\sigma_\varepsilon\right) \tag{11}$$

Using the assumed truncated normal distribution for ε_k, one has

$$p\left(\varepsilon_k\,|\,\mathbf{h},\sigma_\varepsilon\right)=\mathrm{TN}\left(\varepsilon_k\,|\,0,\sigma_k^2\right)=\frac{2}{\sqrt{2\pi}\sigma_\varepsilon}\exp\left(-\frac{\varepsilon_k^2(y_k,\tilde{q}_k\,|\,\mathbf{h})}{2\sigma_\varepsilon^2}\right) \tag{12}$$

with all $\varepsilon_k\geq 0$. Substituting Eq. (12) and (11) into Eq. (10), the posterior distribution takes the form

$$p\left(\mathbf{h},\sigma_\varepsilon\,|\,\varepsilon\right)\propto\frac{1}{\sigma_\varepsilon^{n_q}}\exp\left(-\frac{n_q}{2\sigma_\varepsilon^2}J(\mathbf{h};\{y_k\},\{\tilde{q}_k\})\right)p\left(\mathbf{h}\right)p\left(\sigma_\varepsilon\right) \tag{13}$$

where the notations $\{y_k\}$ and $\{\tilde{q}_k\}$ are defined as the sets $\{y_k\}=\{y_1,\ldots,y_{n_q}\}$ and $\{\tilde{q}_k\}=\{\tilde{q}_1,\ldots,\tilde{q}_{n_q}\}$, and

$$J(\mathbf{h};\{y_k\},\{\tilde{q}_k\})=\frac{1}{n_q}\sum_{k=1}^{n_q}\varepsilon_k^2(y_k,\tilde{q}_k\,|\,\mathbf{h}) \tag{14}$$

is the mean square discrepancy function formed from the individual discrepancies for each measurement property. It should be noted that $J(\mathbf{h};\{y_k\},\{\tilde{q}_k\})$ stabilizes to a finite value as the number of output measured quantities increases. Given the prior distribution, samples $\left\{\mathbf{h}^{(i)},\sigma_\varepsilon^{(i)};i=1,\cdots,n\right\}=\left\{\boldsymbol{\mu}_{\boldsymbol{\theta}}^{(i)},\boldsymbol{\Sigma}_{\boldsymbol{\theta}}^{(i)},\sigma_e^{(i)},\sigma_\varepsilon^{(i)};i=1,\cdots,n\right\}$ of hyper parameters distributed proportional to the joint posterior distribution can be generated by using any sampling algorithm. Herein, the nested sampling algorithm [32] is used to generate samples.

For a large number of output quantities n_q, with the prior distribution $p(\mathbf{h})$ selected to be uniform, Eq. (13) can be approximated as

$$p(\mathbf{h},\sigma_\varepsilon\,|\,\varepsilon)\propto \mathrm{N}\left(\mathbf{h}\,|\,\hat{\mathbf{h}},\sigma_\varepsilon^2\hat{\boldsymbol{\Sigma}}_{\mathbf{h}}\right)p(\sigma_\varepsilon) \tag{15}$$

where $\hat{\mathbf{h}}=\arg\min_{\mathbf{h}}\left[J(\mathbf{h};\{y_k\},\{\tilde{q}_k\})\right]$, $\hat{\boldsymbol{\Sigma}}_{\mathbf{h}}=\frac{1}{n_q}\mathbf{H}^{-1}(\hat{\mathbf{h}})$, $\mathbf{H}(\hat{\mathbf{h}})=\left.\frac{\partial^2 J(\mathbf{h};\{y_k\},\{\tilde{q}_k\})}{\partial\mathbf{h}^{\mathrm{T}}\partial\mathbf{h}}\right|_{\mathbf{h}=\hat{\mathbf{h}}}$. The derivation is given in Appendix A. Noting also that $\mathbf{H}(\hat{\mathbf{h}})$ stabilizes to a finite value as the number of output measured quantities increases, the uncertainty in the estimates of the hyperparameters $\mathbf{h}$ quantified by $\hat{\boldsymbol{\Sigma}}_{\mathbf{h}}$ is inversely proportional to the number of measured variables n_q, which implies that the uncertainty decreases as the number of measured variables increases. For uniform prior PDF $p(\sigma_\varepsilon)$, it can be readily shown using Eq. (A.1) that the most probable value of the parameter σ_ε is given by $\hat{\sigma}_\varepsilon=\sqrt{J(\mathbf{h};\{y_k\},\{\tilde{q}_k\})}$ which is an overall measure of discrepancy between the model predictions and the measurements.

Note that the estimated σ_ε can be used to evaluate the accuracy of the prediction model quantitatively. As ε_k, $k=1,\cdots,n_q$, are assumed to follow a truncated Gaussian distribution with zero mean, σ_ε quantifies the average distance of all KL-div values from zero. So it can be treated as an index of prediction accuracy between the measured and model predicted PDFs. The smaller the value of σ_ε, the better the accuracy.

2.3 Uncertainty quantification of structural model parameters and error term

The posterior distribution of model parameters can be derived using the total probability theorem

$$p(\boldsymbol{\theta}\,|\,\varepsilon)=\int_{\sigma_e}\int_{\sigma_\varepsilon}\int_{\boldsymbol{\mu}_{\boldsymbol{\theta}}}\int_{\boldsymbol{\Sigma}_{\boldsymbol{\theta}}}\mathrm{N}\left(\boldsymbol{\theta}\,|\,\boldsymbol{\mu}_{\boldsymbol{\theta}},\boldsymbol{\Sigma}_{\boldsymbol{\theta}}\right)p\left(\boldsymbol{\mu}_{\boldsymbol{\theta}},\boldsymbol{\Sigma}_{\boldsymbol{\theta}},\sigma_e,\sigma_\varepsilon\,|\,\varepsilon\right)\,d\boldsymbol{\Sigma}_{\boldsymbol{\theta}}\,d\boldsymbol{\mu}_{\boldsymbol{\theta}}\,d\sigma_\varepsilon\,d\sigma_e \tag{16}$$

where use was made of the fact that conditional PDF $p\left(\boldsymbol{\theta}\,|\,\boldsymbol{\mu}_{\boldsymbol{\theta}},\boldsymbol{\Sigma}_{\boldsymbol{\theta}},\sigma_e,\sigma_\varepsilon,\varepsilon\right)=\mathrm{N}\left(\boldsymbol{\theta}\,|\,\boldsymbol{\mu}_{\boldsymbol{\theta}},\boldsymbol{\Sigma}_{\boldsymbol{\theta}}\right)$ depends only on the values of $\boldsymbol{\mu}_{\boldsymbol{\theta}}$ and $\boldsymbol{\Sigma}_{\boldsymbol{\theta}}$. Based on the samples of $\boldsymbol{\mu}_{\boldsymbol{\theta}}$ and $\boldsymbol{\Sigma}_{\boldsymbol{\theta}}$, the integral can be approximated as

$$p(\boldsymbol{\theta}\,|\,\varepsilon)\approx\frac{1}{n}\sum_i^n\mathrm{N}\left(\boldsymbol{\theta}\,|\,\boldsymbol{\mu}_{\boldsymbol{\theta}}^{(i)},\boldsymbol{\Sigma}_{\boldsymbol{\theta}}^{(i)}\right) \tag{17}$$

Similarly, the posterior distribution of the error term is

$$p(e_k\,|\,\varepsilon)=\int_{\sigma_e}\int_{\sigma_\varepsilon}\int_{\boldsymbol{\mu}_{\boldsymbol{\theta}}}\int_{\boldsymbol{\Sigma}_{\boldsymbol{\theta}}}\mathrm{N}\left(e_k\,|\,0,\sigma_e^2\right)p\left(\boldsymbol{\mu}_{\boldsymbol{\theta}},\boldsymbol{\Sigma}_{\boldsymbol{\theta}},\sigma_e,\sigma_\varepsilon\,|\,\varepsilon\right)\,d\boldsymbol{\Sigma}_{\boldsymbol{\theta}}\,d\boldsymbol{\mu}_{\boldsymbol{\theta}}\,d\sigma_\varepsilon\,d\sigma_e \tag{18}$$

where use was made of the fact that $p\left(e_k\,|\,\boldsymbol{\mu}_{\boldsymbol{\theta}},\boldsymbol{\Sigma}_{\boldsymbol{\theta}},\sigma_e,\sigma_\varepsilon,\varepsilon\right)=\mathrm{N}\left(e_k\,|\,0,\sigma_e^2\right)$ depends only on the values of σ_e^2. The integral can be approximated by the following sample estimate

$$p(e_k\,|\,\varepsilon)\approx\frac{1}{n}\sum_i^n\mathrm{N}\left(e_k\,|\,0,\left[\sigma_e^{(i)}\right]^2\right) \tag{19}$$

2.4 Uncertainty propagation to output QoI

Let $z_j\left(\tilde{\boldsymbol{q}}(\boldsymbol{\theta})\right)$, $j=1,\cdots,n_t$ be an output QoI that depends on the quantities $\tilde{\boldsymbol{q}}(\boldsymbol{\theta})=\{\tilde{q}_1(\boldsymbol{\theta}),\ldots,\tilde{q}_{n_q}(\boldsymbol{\theta})\}$. For example, $\tilde{\boldsymbol{q}}(\boldsymbol{\theta})$ can be related to the modal frequencies and mode shape components and $z_j\left(\tilde{\boldsymbol{q}}(\boldsymbol{\theta})\right), j=1,\cdots,n_t$ can be the response time histories (displacement, acceleration, strain, stresses) that are computed from the modal properties using modal analysis. Using samples $\boldsymbol{\theta}^{(l)}$ and $e_k^{(l)}$ generated from the PDFs defined in Eq. (17) and (19), respectively, then the samples of $z_j\left(\tilde{\boldsymbol{q}}(\boldsymbol{\theta})\right)$ can be obtained as $z_j\left(\boldsymbol{q}\left(\boldsymbol{\theta}^{(l)}\right)+\boldsymbol{w}^{(l)}*\boldsymbol{e}^{(l)}\right)$ from which the $\alpha\%$ to $1-\alpha\%$ quantiles of the response QoI can be estimated, where $\boldsymbol{w}^{(l)}*\boldsymbol{e}^{(l)}$ expresses element-wise product. Also the statistics of the response QoI, such as mean and higher moments, can be predicted by the following Monte Carlo estimates

$$\begin{aligned}\mathrm{E}\left[z_j^m\left(\tilde{\boldsymbol{q}}(\boldsymbol{\theta})\right)\right] &= \mathrm{E}\left[z_j^m\left(\boldsymbol{q}(\boldsymbol{\theta})+\boldsymbol{w}*\boldsymbol{e}\right)\right] \\ &= \int_{\boldsymbol{\theta}}\int_{\boldsymbol{e}} z_j^m\left(\boldsymbol{q}(\boldsymbol{\theta})+\boldsymbol{w}*\boldsymbol{e}\right)p(\boldsymbol{\theta}\,|\,\varepsilon)\;p(\boldsymbol{e}\,|\,\varepsilon)\;d\boldsymbol{\theta}\;d\boldsymbol{e} \\ &\approx \frac{1}{n}\sum_{l=1}^{n} z_j^m\left(\boldsymbol{q}\left(\boldsymbol{\theta}^{(l)}\right)+\boldsymbol{w}^{(l)}*\boldsymbol{e}^{(l)}\right)\end{aligned} \tag{20}$$

The mean is given by $\mu_{z_j}=\mathrm{E}\left[z_j\left(\boldsymbol{q}(\boldsymbol{\theta})+\boldsymbol{w}*\boldsymbol{e}\right)\right]$ and the variance by $\sigma_{z_j}^2=\mathrm{E}\left[z_j^2\left(\boldsymbol{q}(\boldsymbol{\theta})+\boldsymbol{w}*\boldsymbol{e}\right)\right]-\mu_{z_j}^2$. Note that for $z_j\left(\boldsymbol{q}(\boldsymbol{\theta})+\boldsymbol{w}*\boldsymbol{e}\right)=q_j(\boldsymbol{\theta})+w_j e_j$, $j=1,\cdots,n_q$, one obtains the predictions of the observed QoI.

3. Application to Structural Dynamics using Measured Modal Properties

For a linear system with n degrees of freedom (DOF), the PDF of measured modal properties are expressed as $\left\{\pi(\hat{f}_r),\ \pi(\hat{\varphi}_{r,j}),\ r=1,2,\ldots,R;\ j=1,2,\ldots,n_0\right\}$, where $\hat{f}_r$ represents the r-th modal frequency, $\hat{\boldsymbol{\phi}}_r=\left[\hat{\varphi}_{r,1},\hat{\varphi}_{r,2},\ldots,\hat{\varphi}_{r,n_0}\right]$ is the r-th normalized mode shape vector at n_0 measured locations, and R is the number of contributed modes. Treating each modal property to be a model output, as there are R modal frequencies and $R\times n_0$ mode shapes, the number of model outputs is $R\times(n_0+1)$. Consider a model parameterized by $\boldsymbol{\theta}$, the model outputs corresponding to the measurements are $\left\{f_r(\boldsymbol{\theta}),\boldsymbol{\phi}_r(\boldsymbol{\theta}),r=1,2,\ldots,R\right\}$, and the predictions from the model that take into account model errors are defined as

$$\begin{aligned}\tilde{f}_r(\boldsymbol{\theta}) &= f_r(\boldsymbol{\theta})+w_r e_r \\ \tilde{\varphi}_{r,j}(\boldsymbol{\theta}) &= \varphi_{r,j}(\boldsymbol{\theta})+w_{r,j}e_{r,j}\end{aligned} \tag{21}$$

where e_r and $e_{r,j}$ are assigned to follow an identical Gaussian distribution $\mathrm{N}\left(0,\sigma_e^2\right)$. To take into account the different intensities of the modal frequencies and the mode shape components, the weight factors w_r and $w_{r,j}$ are respectively selected to be the mean of $\hat{f}_r$ and $\hat{\varphi}_{r,j}$.

Based on the measurements and probabilistic model described above, the proposed probabilistic modeling framework can be implemented. The posterior distribution of hyper parameters is given by Eq. (13) where the discrepancy function in Eq. (14) becomes

$$J(\mathbf{h};\{y_k\},\{\tilde{q}_k\}) = \frac{1}{R(n_0+1)}\left[\sum_{r=1}^{R}\varepsilon_r^2(\hat{f}_r,\tilde{f}_r\,|\,\mathbf{h}) + \sum_{r=1}^{R}\sum_{j=1}^{n_0}\varepsilon_{r,j}^2(\hat{\varphi}_{r,j},\tilde{\varphi}_{r,j}\,|\,\mathbf{h})\right] \tag{22}$$

and $n_q = R(n_0+1)$. Approximating the PDFs $\pi(\hat{f}_r)$ and $\pi(\hat{\varphi}_{r,j})$ by Gaussian distributions, the formula of KL-div can be simplified using Eq. (8), so that the expressions $\varepsilon_r(\{\hat{f}_r\},\{\tilde{f}_r\}\,|\,\mathbf{h})$ and $\varepsilon_{r,j}(\{\hat{\varphi}_{r,j}\},\{\tilde{\varphi}_{r,j}\}\,|\,\mathbf{h})$ depend on the mean and variances of the model predictions conditional on the values of the hyperparameters $\mathbf{h}$, given by

$$\begin{aligned}
\mu_{\tilde{f}_r|\mathbf{h}} &= \int_{\mathbf{h}}\left[\, f_r(\boldsymbol{\theta}) + w_r e_r \,\right] p(\boldsymbol{\theta}\,|\,\mathbf{h})\, p(e_r\,|\,\mathbf{h})\, d\mathbf{h} = \int_{\mathbf{h}} f_r(\boldsymbol{\theta})\, p(\boldsymbol{\theta}\,|\,\mathbf{h})\, d\mathbf{h} = \mu_{f_r|\mathbf{h}} \\
\sigma^2_{\tilde{f}_r|\mathbf{h}} &= \int_{\mathbf{h}}\left[\, f_r(\boldsymbol{\theta}) + w_r e_r - \mu_{\tilde{f}_r|\mathbf{h}} \,\right]^2 p(\boldsymbol{\theta}\,|\,\mathbf{h})\, p(e_r\,|\,\mathbf{h})\, d\mathbf{h} = \int_{\mathbf{h}}\left[\, f_r(\boldsymbol{\theta}) - \mu_{f_r|\mathbf{h}} \,\right]^2 p(\boldsymbol{\theta}\,|\,\mathbf{h})\, d\mathbf{h} + w_r^2\sigma_e^2 \\
\mu_{\tilde{\varphi}_{r,j}|\mathbf{h}} &= \int_{\mathbf{h}}\left[\, \varphi_{r,j}(\boldsymbol{\theta}) + w_{r,j} e_{r,j} \,\right] p(\boldsymbol{\theta}\,|\,\mathbf{h})\, p(e_{r,j}\,|\,\mathbf{h})\, d\mathbf{h} = \int_{\mathbf{h}} \varphi_{r,j}(\boldsymbol{\theta})\, p(\boldsymbol{\theta}\,|\,\mathbf{h})\, d\mathbf{h} = \mu_{\varphi_{r,j}|\mathbf{h}} \\
\sigma^2_{\tilde{\varphi}_{r,j}|\mathbf{h}} &= \int_{\mathbf{h}}\left[\, \varphi_{r,j}(\boldsymbol{\theta}) + w_{r,j} e_{r,j} - \mu_{\tilde{\varphi}_{r,j}|\mathbf{h}} \,\right]^2 p(\boldsymbol{\theta}\,|\,\mathbf{h})\, p(e_{r,j}\,|\,\mathbf{h})\, d\mathbf{h} \\
&= \int_{\mathbf{h}}\left[\, \varphi_{r,j}(\boldsymbol{\theta}) - \mu_{\varphi_{r,j}|\mathbf{h}} \,\right]^2 p(\boldsymbol{\theta}\,|\,\mathbf{h})\, d\mathbf{h} + w_{r,j}^2\sigma_e^2
\end{aligned} \tag{23}$$

To calculate the multi-dimensional integrals efficiently, the univariate dimension reduction method (UDRM) [33] is introduced to approximate them. The UDRM involves an additive decomposition of a multivariate response function into multiple univariate functions, so the multi-dimensional integral required by response moments are approximated by a series of one-dimensional integral of these univariate functions. According to UDRM, $f_r(\boldsymbol{\theta})$ and $\varphi_{r,j}(\boldsymbol{\theta})$ can be approximated as

$$\begin{aligned}
f_r(\boldsymbol{\theta}) &\approx -(n-1)\, f_r(\boldsymbol{\mu}_{\boldsymbol{\theta}}) + \sum_{i=1}^{n} f_r\left(\theta_i, \boldsymbol{\mu}_{\boldsymbol{\theta}_{-i}}\right) \\
\varphi_{r,j}(\boldsymbol{\theta}) &\approx -(n-1)\,\varphi_{r,j}(\boldsymbol{\mu}_{\boldsymbol{\theta}}) + \sum_{i=1}^{n} \varphi_{r,j}\left(\theta_i, \boldsymbol{\mu}_{\boldsymbol{\theta}_{-i}}\right)
\end{aligned} \tag{24}$$

where $\boldsymbol{\mu}_{\boldsymbol{\theta}_{-i}}$ represents the mean vector of $\boldsymbol{\theta}\in\mathbb{R}^n$ that excludes the component μ_{θ_i}, and $f_r\left(\theta_i, \boldsymbol{\mu}_{\boldsymbol{\theta}_{-i}}\right)$ is defined as $f_r\left(\theta_i, \boldsymbol{\mu}_{\boldsymbol{\theta}_{-i}}\right) = f_r\left(\mu_{\theta_1}, \mu_{\theta_2}, \cdots, \mu_{\theta_{i-1}}, \theta_i, \mu_{\theta_{i+1}}, \cdots, \mu_{\theta_n}\right)$. Substituting Eq. (24) into Eq. (23), the mean and variance can be approximated into a series of one-dimensional integral of univariate functions in Eq. (24) [33], which can be easily solved by numerical integral methods, hereby a lot of computation can be saved.

4. Simulated Example

A population of 3-DOF linear systems manufactured to be identical is taken as a simulated example. Due to manufacturing variabilities, the properties of the system, such as stiffness vary for each member in the population. The modal properties of the members of the population are chosen as measured quantities to study the effectiveness of the proposed probabilistic modeling framework.

4.1 Model description

Consider a three DOF model, shown in Figure 2, introduced to represent each member in the population. The nominal values of the mass for the model DOFs are set to be $m_1 = 6\text{kg}$, $m_2 = 5\text{kg}$ and $m_3 = 5\text{kg}$, while the nominal values of the stiffness of each link are set to $k_{10} = 22\text{kN/m}$, $k_{20} = 21\text{kN/m}$ and $k_{30} = 20\text{kN/m}$. With these assumptions, the modal properties of the nominal model are listed in Table 1.

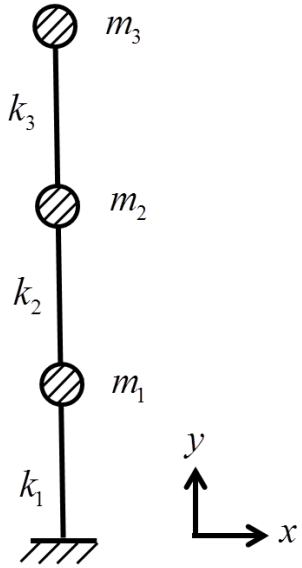

Figure 2 3-DOF spring mass chain system

Table 1 Modal properties

	Frequency (Hz)	**Mode shape at DOF 1**	**Mode shape at DOF 2**	**Mode shape at DOF 3**
Mode 1	4.59	0.324	0.587	0.741
Mode 2	12.2	0.740	0.281	-0.611
Mode 3	17.9	-0.498	0.787	-0.362

4.2 Uncertainty quantification

The properties of each member in the population are simulated as follows. To consider the variation of model parameters from member to member due to manufacturing variability, the stiffness of the link i of each member is generated from a Gaussian distribution $k_i(x) \sim N\left(x \mid k_{i0}, (k_{i0} * 0.03)^2\right)$, $i = 1, 2, 3$, corresponding to approximately 3% variation of the stiffness parameters about their nominal values. The modal properties are then simulated from Eq. (21) using 10^3 MCs samples. The error terms defined in Eq. (21) are assumed to follow the Normal distribution with zero mean and standard deviation equals to 0.05, corresponding to a 5% model error. The mean and variance of modal properties are then computed and listed in Table 2 serving as known statistics of measurements. Then the uncertainty quantification for the stiffness parameters can be conducted according to the methodology presented in Section 3.

Table 2 Mean and variance of simulated modal properties

	Frequency		**Mode shape at DOF 1**		**Mode shape at DOF 2**		**Mode shape at DOF 3**	
	mean	variance	mean	variance	mean	variance	mean	variance
Mode 1	4.59	0.015	0.324	3.1×10^{-4}	0.587	8.8×10^{-4}	0.741	1.4×10^{-3}
Mode 2	12.2	0.106	0.740	1.5×10^{-3}	0.281	5.4×10^{-4}	-0.611	9.8×10^{-4}
Mode 3	17.9	0.233	-0.498	8.3×10^{-4}	0.787	1.6×10^{-3}	-0.362	5.2×10^{-4}

The 3-DOF model shown in Figure 2 is used to represent each member in the group. To take into account the variation in the model properties, the stiffness of each link is parameterized by $\boldsymbol{\theta}=\left[\theta_1\ \theta_2\ \theta_3\right]^{\mathrm{T}}$ such as $k_i\left(\theta_i\right)=k_{i0}*\theta_i$, where $\boldsymbol{\theta}$ are model parameters to be identified. Assuming the prior distributions of all the hyper parameters to be uniform distributions with their upper and lower boundaries listed in Table 3, the nested sampling algorithm [32] is implemented to generate samples of hyper parameters. The results are shown in Figure 3, while the mean and standard deviation of the posterior distributions of hyper parameters are summarized in Table 4. As expected, the estimated mean values of all the hyper parameters $\boldsymbol{\mu}_{\boldsymbol{\theta}}$ and $\boldsymbol{\Sigma}_{\boldsymbol{\theta}}$ (defined to be diagonal), as well as the prediction error parameter σ_e, show good agreement with the nominal values used to simulate the measurements. The standard deviations of the hyperparameters are small, which means the uncertainty of identified results is small. Also, the values of the samples for σ_ε are very small, which means the prediction results have a good accuracy compared with measurements. The closeness of the results to the values used to simulate the measurements also demonstrates that the Gaussian approximation of modal properties assumed in Section 3 is reasonable.

Table 3 Upper and lower boundaries of hyper parameters

	μ_{θ_1}	σ_{θ_1}	μ_{θ_2}	σ_{θ_2}	μ_{θ_3}	σ_{θ_3}	σ_e	σ_ε
Upper boundary	0.8	0	0.8	0	0.8	0	0	0
Lower boundary	1.2	0.1	1.2	0.1	1.2	0.1	0.1	1

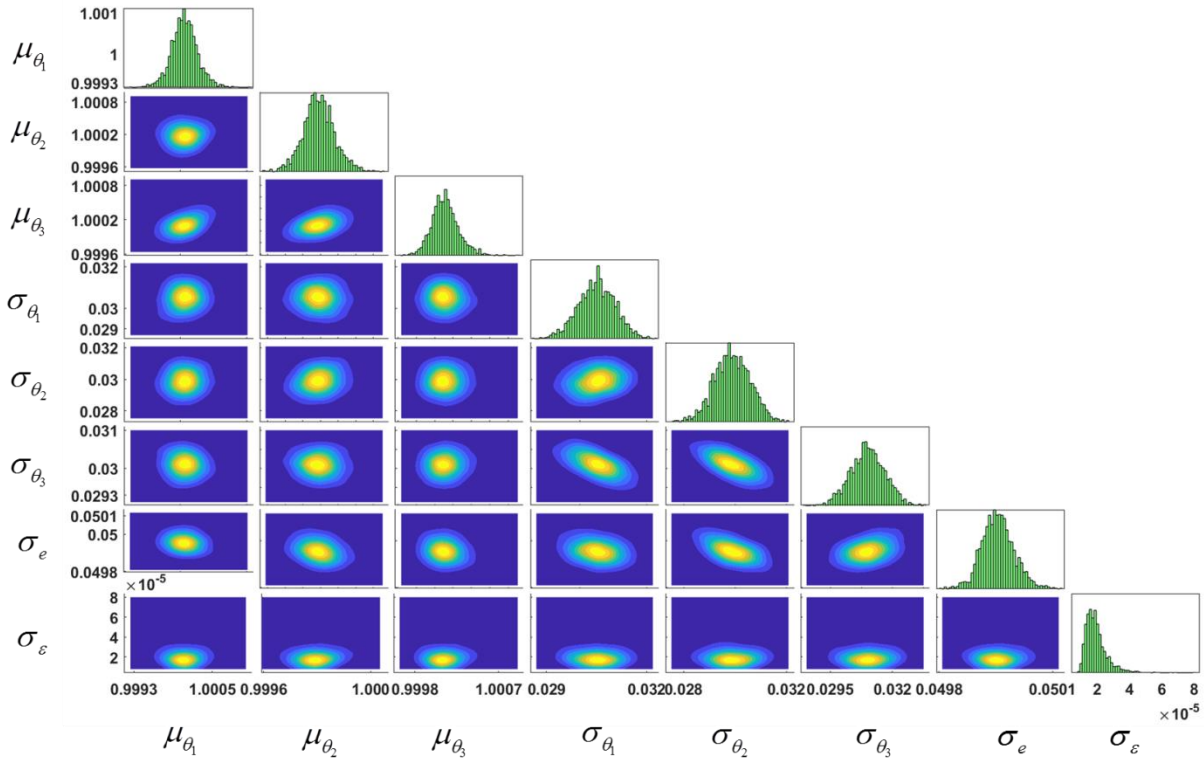

Figure 3 Samples of joint posterior distribution of hyper parameters

Table 4 Estimates of mean and standard deviation of hyper parameters

	μ_{θ_1}	μ_{θ_2}	μ_{θ_3}	σ_{θ_1}	σ_{θ_2}	σ_{θ_3}	σ_e
Nominal value	1	1	1	0.03	0.03	0.03	0.05
Mean	1.0001	1.0002	1.0001	0.0305	0.0299	0.0301	0.0500
Standard deviation	2.1×10^{-4}	2.2×10^{-4}	2.1×10^{-4}	6×10^{-4}	7×10^{-4}	3×10^{-4}	5×10^{-5}

Based on Eq. (16) and (18), the posterior distributions of $\boldsymbol{\theta}$ and $e_r, e_{r,j}$ are computed using sampling and shown in Figure 4. As $e_r, e_{r,j}$ are identically distributed, there is only one figure for their posterior distribution. The estimated statistics of $\boldsymbol{\theta}$ and e are summarized in Table 5. The values are compared with the nominal values assigned to simulate the measurements. It can be seen that the mean and standard deviation of posterior distributions of model parameters and error terms are very close to the nominal values. The samples of ε are close to zeros, which indicates that the discrepancy between the PDFs of measurements and predictions is small enough.

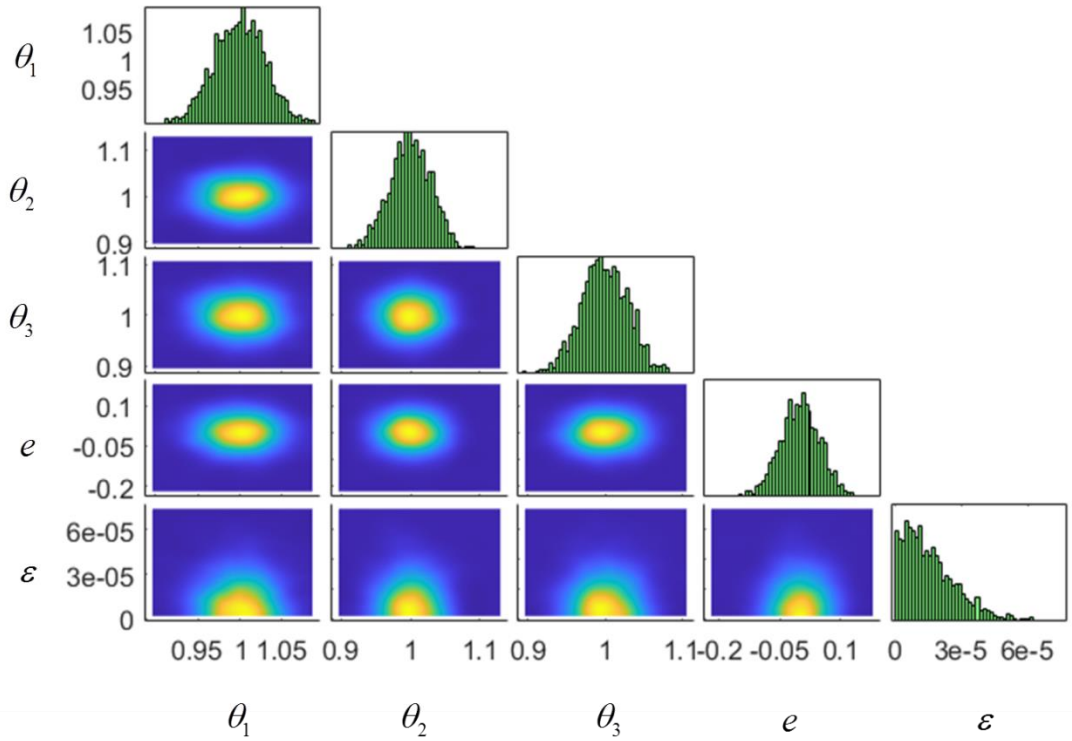

Figure 4 Samples of posterior distribution of $\boldsymbol{\theta}$, $e=\left\{e_r, e_{r,j};, r=1,2,\cdots,R;, j=1,2,\cdots,n_0\right\}$ and ε

Table 5 Estimates of mean and standard deviation of model parameters and error terms

	θ_1	θ_2	θ_3	e
Mean	1.0010	1.0010	1.0000	-0.0012
Standard deviation	0.0307	0.0293	0.0301	0.0494

4.3 Uncertainty propagation

Using the samples of $\boldsymbol{\theta}$, e_r and $e_{r,j}$, the mean and variance of modal properties are predicted and listed in Table 6. These values should be compared with the mean and variance of the measurements in Table 2. The predicted results are of good accuracy, and the maximum relative error is less than 4%. The predicted PDFs of modal properties are also computed and compared with Gaussian PDFs of the measurements in Figure 5. A very good agreement is also observed, validating the effectiveness of the proposed methodology in identifying the model parameters. It should be noted that such uncertainty bounds are expected to be thin for classical Bayesian framework based on multiple datasets used for the modal properties [34]. The level of uncertainty is expected in classical Bayesian approaches to decrease as the number of data increases.

Table 6 Predicted mean and variance of the modal properties

	Frequency		**Mode shape at DOF 1**		**Mode shape at DOF 2**		**Mode shape at DOF 3**	
	mean	variance	mean	variance	mean	variance	mean	variance
Mode 1	4.59	0.015	0.324	3.1×10^{-4}	0.587	8.8×10^{-4}	0.743	1.4×10^{-3}
Mode 2	12.2	0.107	0.741	1.5×10^{-3}	0.280	5.7×10^{-4}	-0.611	9.7×10^{-4}
Mode 3	17.9	0.225	-0.498	8.4×10^{-4}	0.787	1.6×10^{-3}	-0.363	5.0×10^{-4}

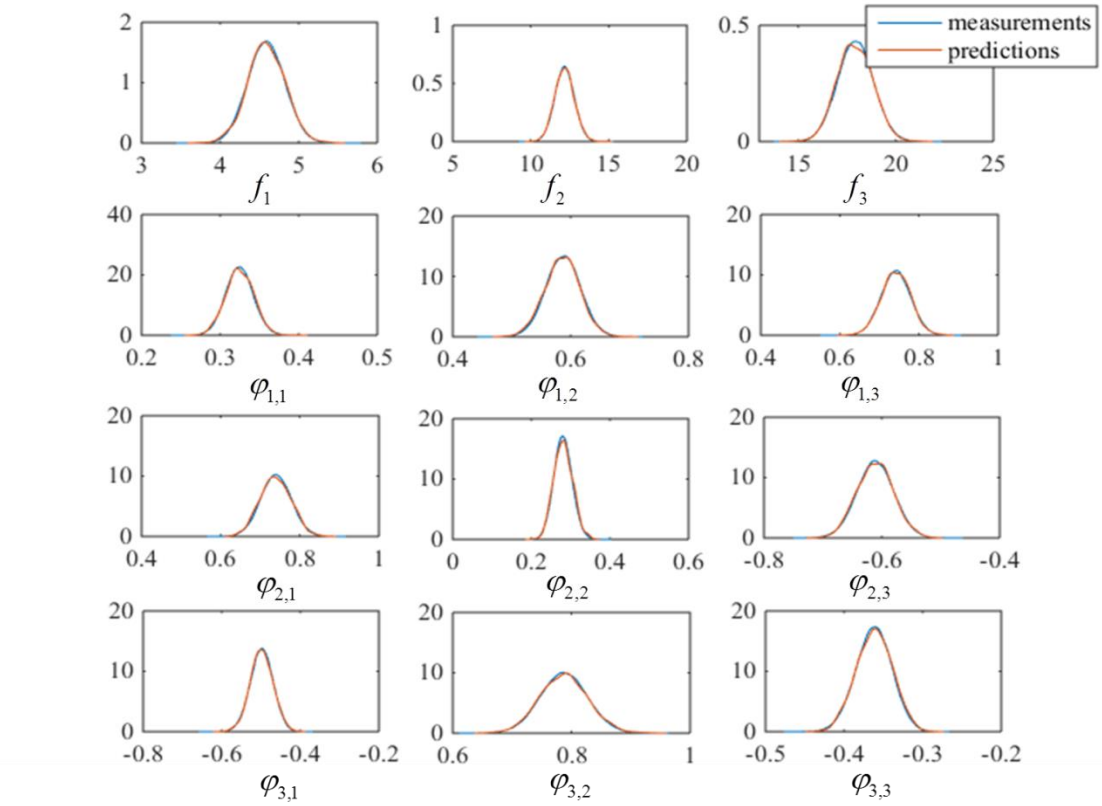

Figure 5 Comparison between measured and predicted PDFs for the modal properties

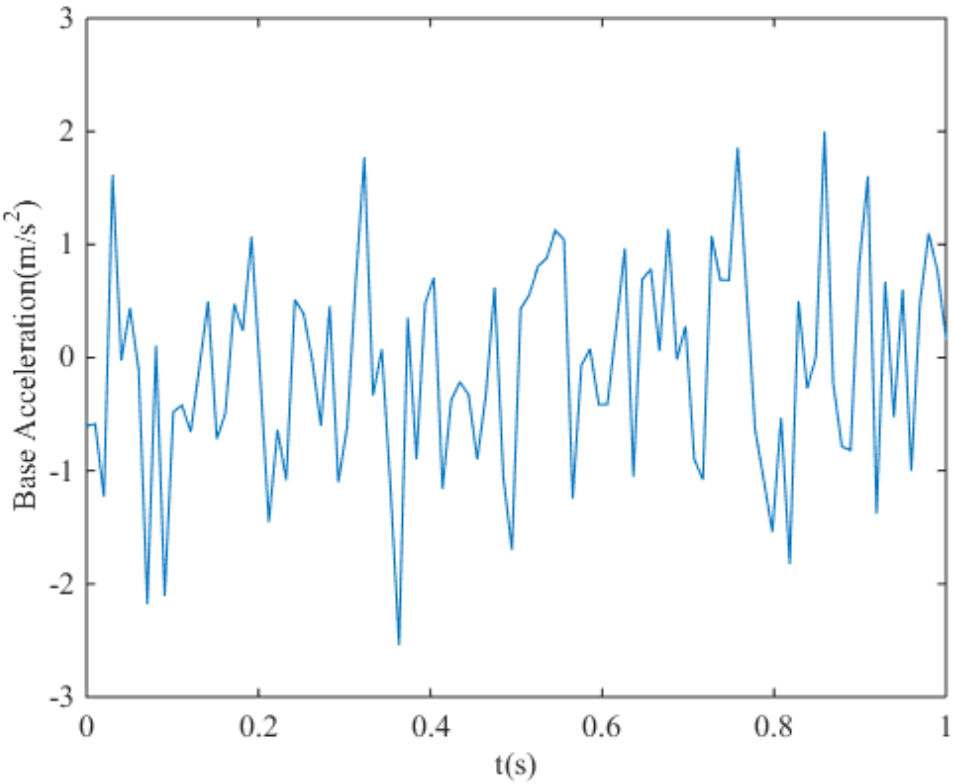

Figure 6 Base excitation

Furthermore, based on the identified modal properties, the response time history of displacement or acceleration or velocity can also be predicted. For this, a zero mean discrete Gaussian white noise base excitation with standard deviation 1, shown in Figure 6, is applied and the mean and variance of time history response of displacement of the third DOF is estimated taking into account the uncertainties in the model parameters and error terms assumed to simulate the measurements in Section 4.2. The modal analysis is used to perform the corresponding predictions based on the predicted modal properties with error terms taken into consideration. To make a comparison, the mean and 90% credible interval boundaries obtained respectively from measurements and predictions are shown in Figure 7. As we can see, the model prediction results match very well the measurements. For the situation that the error terms of modal properties are not considered in the predictions the predicted uncertainty intervals are smaller than that of measurement uncertainty intervals, as shown in Figure 8, signifying that the error terms are necessary to be included in the propagation analysis for accurate model predictions.

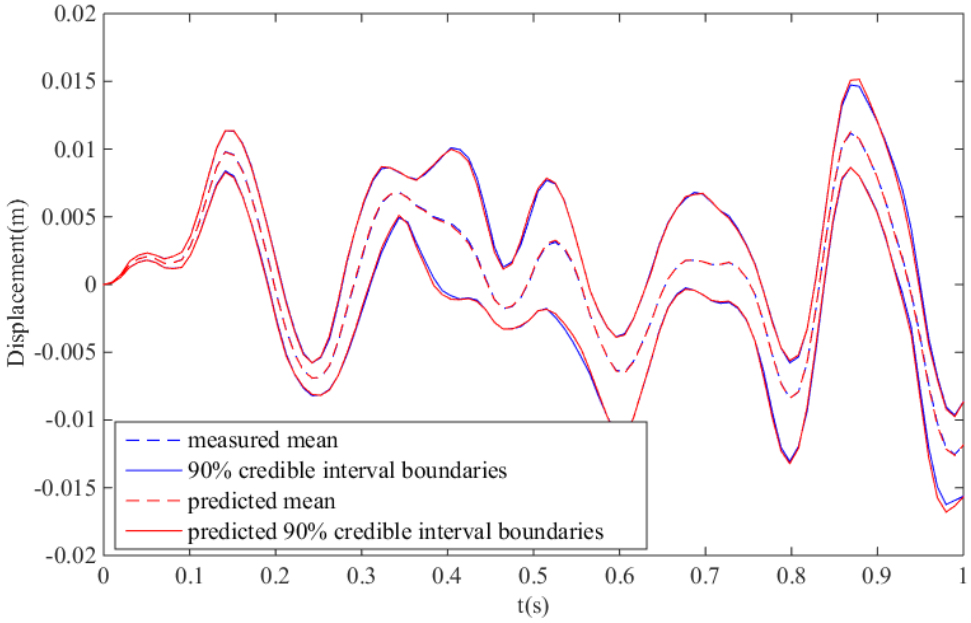

Figure 7 Comparison between measured and predicted results for the displacement time history at DOF 3

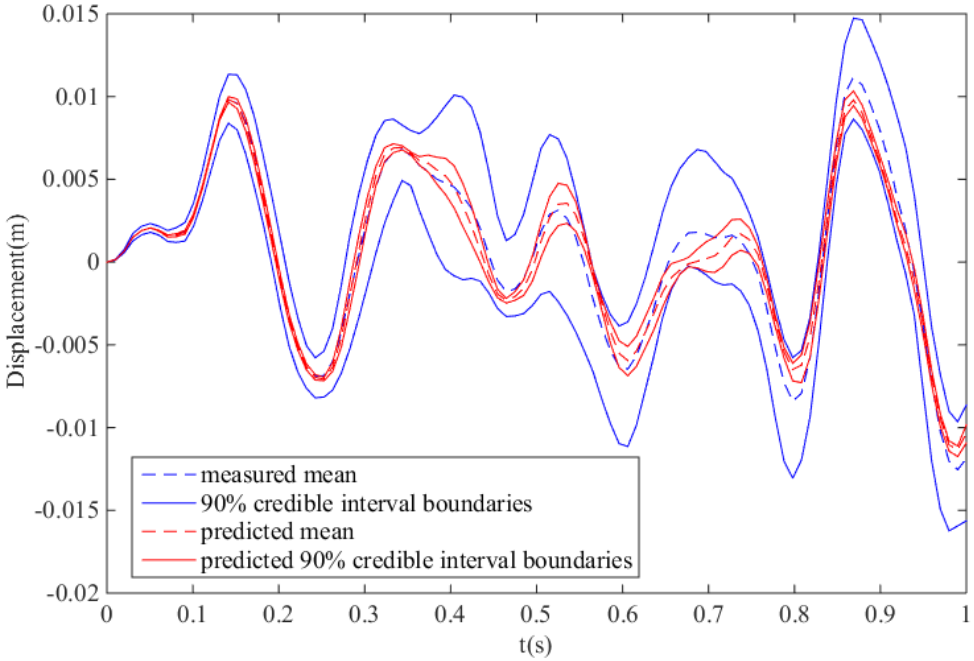

Figure 8 Comparison between measured and predicted results for the displacement time history at DOF 3 without consideration of error terms in prediction

5. Estimation of S-N Curve Model Parameters using Fatigue Data

In this section, the experimental data from fatigue tests are used to infer the uncertainties in the model parameters of the *S-N* curves. As the *S-N* data is usually modelled by a linear model, the equations derived for the linear model in Section 2.1 are directly applicable.

5.1 Model description

Materials fatigue performance is commonly characterized in the form of an *S-N* curve,

which is usually simulated by the Basquin's relation [35]

$$N_k = AS_k^{-B} \tag{25}$$

where N_k expresses the fatigue life at the k-th stress level, S_k expresses corresponding stress level, while $A>0$ and $B>0$ are material parameters to be estimated using experimental data. For the laboratory fatigue tests, the fatigue life dispersion always exists due to many factors, such as uncertainties of mechanical properties of structure and material, changing environmental factors in laboratory, and random error in observations, etc. Taking the variability into consideration, Eq. (25) can be expressed as

$$N_k = AS_k^{-B}\eta_k \tag{26}$$

where η_k quantifies the randomness of fatigue life in stress level S_k. For the sake of simplicity, Eq. (26) is usually rewritten in log scale as [36]

$$\tilde{q}_k = \alpha + \beta x_k + e_k \tag{27}$$

where $\tilde{q}_k = \log_{10}(N_k)$, $x_k = \log_{10} S_k - \frac{1}{n}\sum_{j=1}^{n}\log_{10} S_j$, $\alpha = \log_{10}(A) - B\frac{1}{n}\sum_{j=1}^{n}\log_{10} S_j$, $\beta = B$, and $e_k = \ln\eta_k$ is assumed to follow a zero mean normal distribution with dispersion σ.

Eq. (27) is usually adopted as a probabilistic model to estimate probabilistic *S-N* curves. To consider the variability of the model parameter set $\boldsymbol{\theta} = \{\alpha, \beta\}$ for different specimens, the parameters α and β are respectively assumed to follow Gaussian distributions as $\mathrm{N}\left(\alpha \mid \mu_\alpha, \sigma_\alpha^2\right)$ and $\mathrm{N}\left(\beta \mid \mu_\beta, \sigma_\beta^2\right)$, where μ_α, σ_α, μ_β and σ_β are the hyperparameters. To avoid unidentifiability issues with respect to the model parameters σ_α and σ due to the presence of the additive terms $\alpha + e_k$ in Eq. (27), the term e_k and its uncertainty is absorbed in α by replacing Eq. (27) with the model

$$\tilde{q}_k = \alpha + \beta x_k \tag{28}$$

Based on this model, both the variability of different specimens in one stress level and across stress levels can be comprehensively considered in σ_α and σ_β.

5.2 Uncertainty quantification using fatigue tests

The data listed in Table 7, taken from [37], are used to infer the model parameters. Fatigue tests were conducted with standard plate specimens of aluminum alloy 2524-T3 under four stress levels with about 15 observations each. The data from each stress level is assumed to follow a Gaussian distribution, and the mean and standard deviation are solved as measured statistics. Based on the probabilistic model described above, the proposed probabilistic modeling framework can be implemented. Given the prior distributions of all the hyper parameters as uniform distribution with their upper and lower bounds listed in Table 8, the nested sampling algorithm is implemented to generate samples of the hyper parameters $\{\mu_\alpha, \sigma_\alpha, \mu_\beta, \sigma_\beta\}$ as shown in Figure 9. Moreover, the most probable values of $\{\mu_\alpha, \sigma_\alpha, \mu_\beta, \sigma_\beta\}$ computed according to Eq. (A.3), as well as the standard deviation of the estimates of the hyper-parameters computed using the samples, are listed in Table 9. Based on Eq. (17), the posterior distribution of α and β are shown in Figure 10. Using the samples in Figure 9, the uncertainties in the estimates of the hyperparameters are of the order of 0.83% and 12% for the hyper-mean parameters $\{\mu_\alpha, \mu_\beta\}$ and of the order of 46% and 70% for the hyper-standard deviation parameters $\{\sigma_\alpha, \sigma_\beta\}$. Also, from Table 9 the coefficient of variation

of the parameters α and β based on the mean values of the hyper parameters are $\hat{\sigma}_\alpha / \hat{\mu}_\alpha = 1.7\%$ and $\hat{\sigma}_\beta / \hat{\mu}_\beta = 21\%$, respectively. It can be seen that there is considerable uncertainty in the values of the parameters α and β that can affect fatigue predictions.

Table 7 Fatigue life test data of aluminum alloy 2524-T3

S_i (MPa)	$\log_{10} N_i$
200	5.603, 5.544, 5.528, 5.630, 5.594, 5.540, 5.581, 5.548, 5.426, 5.567, 5.554, 5.627, 5.630, 5.596, 5.626
300	5.028, 5.074, 5.016, 4.894, 4.993, 5.071, 5.024, 5.035, 4.954, 5.039, 5.098, 5.057, 5.092, 5.082, 5.005
350	4.784, 4.842, 4.776, 4.813, 4.813, 4.860, 4.798, 4.776, 4.758, 4.770, 4.755, 4.837, 4.736, 4.842, 4.796
400	4.477, 4.400, 4.426, 4.462, 4.592, 4.411, 4.447, 4.402, 4.665, 4.475, 4.458, 4.551, 4.525, 4.641

Table 8 Upper and lower bounds of hyper parameters

	μ_α	σ_α	μ_β	σ_β	σ_ε
Upper bound	-30	-30	0	0	0
Lower bound	30	30	10	10	10

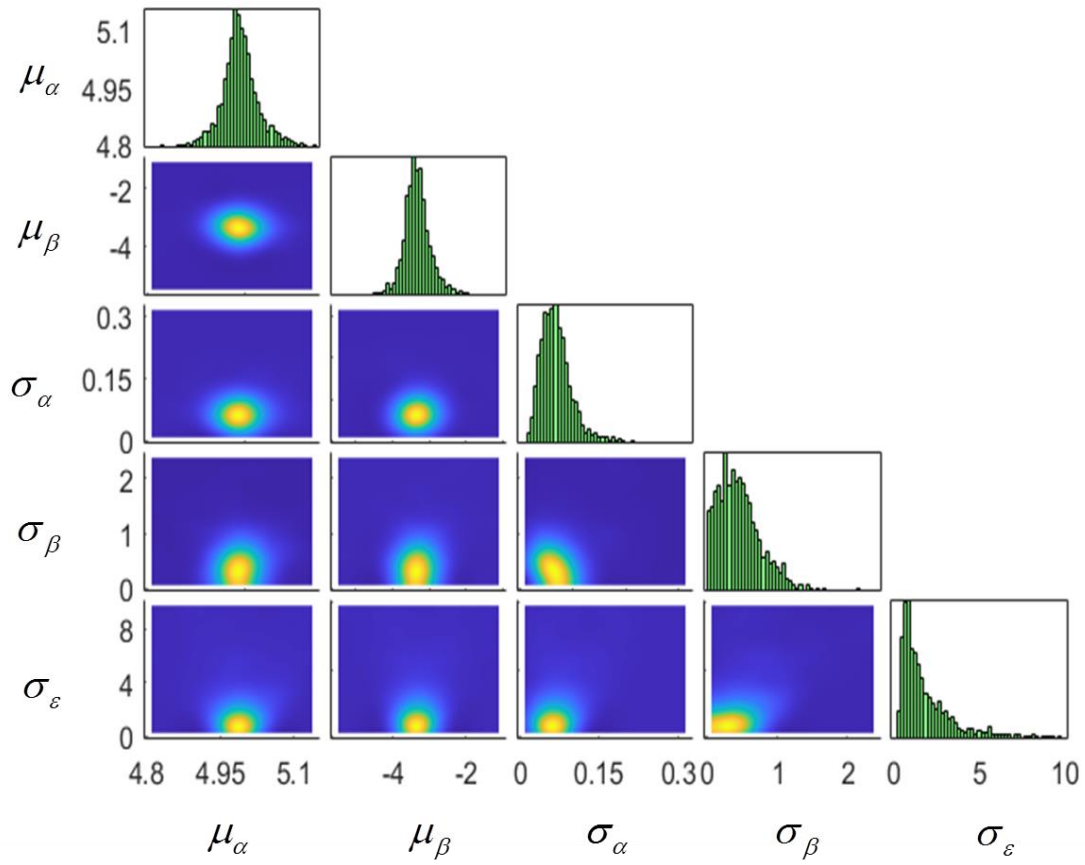

Figure 9 Samples of joint posterior distribution of hyper parameters

Table 9 Most probable values of hyper parameters

	μ_α	μ_β	σ_α	σ_β	σ_ε
MPV	4.984	-3.435	0.511	0.372	0.387
Standard deviation	0.0127	0.1533	0.0166	0.1958	0.1367

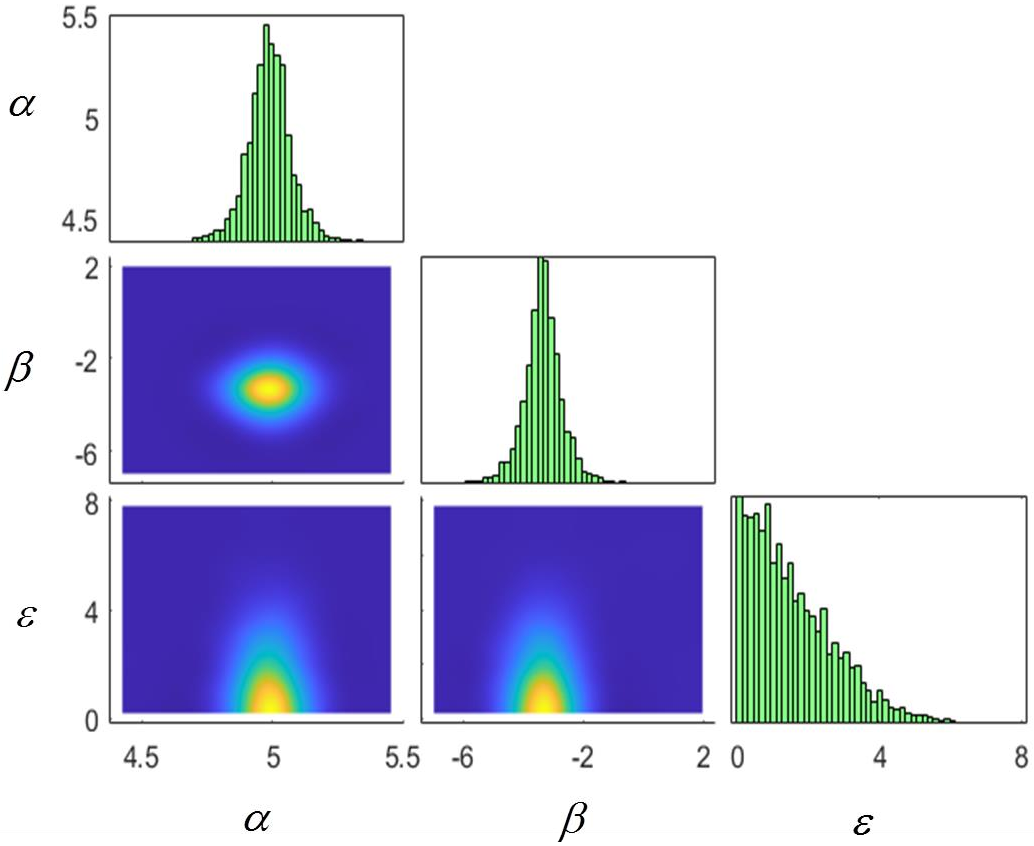

Figure 10 Samples of posterior distribution of α, β and ε

5.3 Uncertainty propagation

Using the samples of α and β generated by Eq. (17), the samples of q_k for various stress levels are predicted and the 90% credible interval is estimated. Results are shown in Figure 11 and compared with measured data available for the four stress levels. Predictions of the 90% credible intervals take into account the uncertainty in the hyper-parameters. Results are also presented for the 90% credible intervals estimated by ignoring the uncertainties in the hyper-parameters. This is achieved by drawing samples from the distribution $\mathrm{N}\left(\boldsymbol{\theta}\,|\,\hat{\boldsymbol{\mu}}_{\boldsymbol{\theta}}, \hat{\boldsymbol{\Sigma}}_{\boldsymbol{\theta}}\right)$ and propagating these samples for predicting the fatigue life for different stress levels in Figure 11. It can be seen that the 90% uncertainty intervals considering the uncertainties in the hyper parameters are narrow enough and contain the fatigue data available at the four stress levels. Moreover, these uncertainty intervals are comparable to uncertainty intervals obtained by methods based on HBM [38,39]. The uncertainty intervals computed using the MPV of the hyper parameters, ignoring the uncertainties in the hyper parameters, are narrower and contain well a large percentage of fatigue data. It is evident, however, that propagation based on the MPV of the hyper parameters fail to fully contain all the data. The discrepancy between the

two credible intervals is expected to decrease as one includes fatigue data from more than four stress levels.

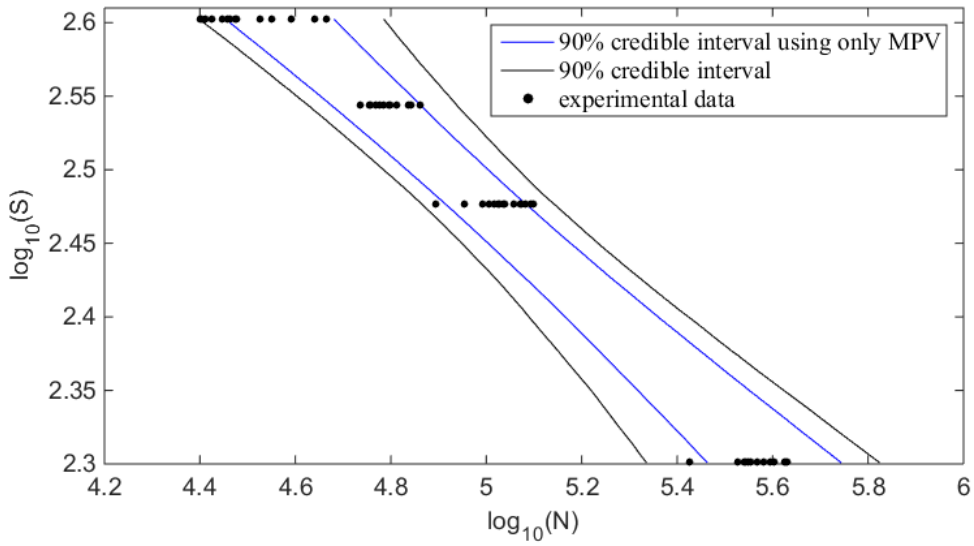

Figure 11 Predicted 90% credible intervals and comparison with measured fatigue data

Finally, from the results in Figure 9, it is observed that the values of σ_ε are not close to zero, which means there are some discrepancies between predicted PDFs and the measured PDFs. This is also depicted in Figure 11, as well as in Figure 12 comparing, for each stress level, the prediction of the Gaussian PDF of q_k based on the model to the Gaussian PDF based on the measurements. For the model predictions, the PDF corresponding to the most probable values of the hyperparameters is presented along with the PDF taking into account the uncertainties in the hyper parameters. It can be seen that the most probable values of two PDFs in each figure are consistent, while the uncertainty predicted using only MPV is narrower than that considering uncertainties of hyper parameters. The reason for the discrepancies between measured and model predicted PDFs is that the variation of the available fatigue data from the four stress levels deviates from the linear model, so that the predictions from the linear model cannot exactly account for the mean and variance of experimental data for all four stress levels simultaneously.

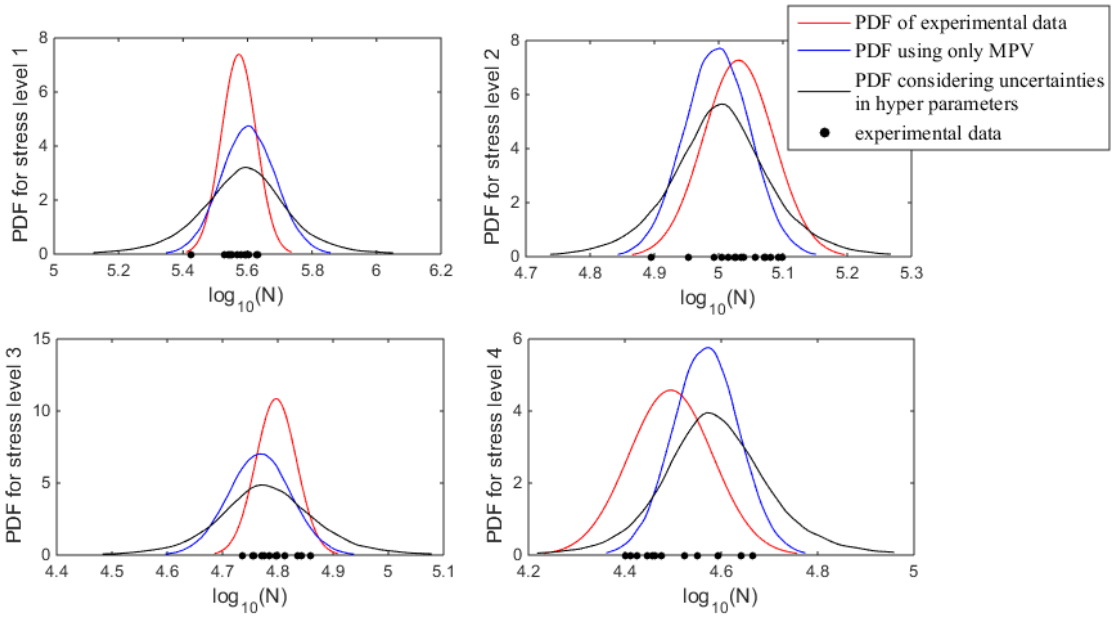

Figure 12 Comparison of PDF of experimental data and model predicted PDFs for the four stress levels

6. Conclusion

The new Bayesian inference method proposed in this work addresses the issue of underestimation of the uncertainty in the model parameters due to model error, mentioned in [24], arising from multiple measurements available for a structure or measurements available for members of a population of identically manufactured structures [18,19]. The proposed method offers an alternative to HBM methods recently proposed in the literature [21,2525] to correctly address the uncertainty in the model parameters. Based on the proposed framework, uncertainties are embedded in the model parameters by assigning a Normal distribution with mean and covariance constituting the hyperparameters to be estimated using Bayesian inference. The posterior distribution of hyper parameters of the model parameters is directly computed by Bayes theorem applied on KL-div measures between the model predicted PDF and the PDF of the experimental data. In particular, the proposed framework is applicable when the statistics of the measured quantities are available. Computationally efficient and insightful analytical expressions for the posterior distribution of the hyperparameters were developed for the case for which the PDFs are approximated by Normal distributions. In particular, Normal distributions for the predictions arise when the output QoI depend linearly on the model parameters. In this case the posterior PDF of the model parameters depends on the lower two moments of the respective PDFs. This representation of the posterior is also used for non-Gaussian PDFs to approximate the uncertainty in the model parameters. For nonlinear relations between the output QoI and the model parameters, the univariate dimension reduction method (UDRM) is used to efficiently estimate the involved multi-dimensional integrals for the lower two moments of model predicted PDF.

An application to structural dynamics based on measured modal properties from a group of identically manufactured 3-DOF systems is presented based on simulated data to illustrate the proposed framework. The effectiveness of the methodology is demonstrated by noting that the estimates of hyperparameters, model parameters, and uncertainties recover the values used to simulate the data. Also, the method is applied to the quantification of uncertainties of the parameters of *S-N* curves based on the experimental data from fatigue tests, demonstrating that the proposed framework can also obtain competitive results to alternative methods based on HBM.

Acknowledgements
This project has received funding from the European Union's Horizon 2020 research and innovation programme under the Marie Skłodowska-Curie grant agreement No 764547. The first author wishes to gratefully acknowledge financial support from China Scholarship Council.

Appendix A

Introduce the function $L(\mathbf{h},\sigma_\varepsilon)$ defined as the negative of the logarithm of the posterior distribution in Eq. (13)

$$L(\mathbf{h},\sigma_\varepsilon) = -\ln p(\mathbf{h},\sigma_\varepsilon \mid \varepsilon) = n_q \ln \sigma_\varepsilon + \frac{n_q}{2\sigma_\varepsilon^2} J(\mathbf{h};\{y_k\},\{\tilde{q}_k\}) \tag{A.1}$$

where the prior PDF $p(\mathbf{h})$ is assumed to be uniform. Using Taylor series expansion with respect to variables $\mathbf{h}$ about the most probable value $\hat{\mathbf{h}}$ of $p(\mathbf{h},\sigma_\varepsilon \mid \varepsilon)$, given by

$$\hat{\mathbf{h}} = \arg\min_{\mathbf{h}} \left[J(\mathbf{h};\{y_k\},\{\tilde{q}_k\}) \right] \tag{A.2}$$

and keeping the first two non-zero terms in the expansion, the posterior PDF $p(\mathbf{h},\sigma_\varepsilon \mid \varepsilon) = \exp\left(-L(\mathbf{h},\sigma_\varepsilon)\right)$ can be approximated as (valid for larger number of output quantities)

$$p(\mathbf{h},\sigma_\varepsilon \mid \varepsilon) \propto p(\sigma_\varepsilon)\, \mathrm{N}\left(\mathbf{h} \mid \hat{\mathbf{h}}, \sigma_\varepsilon^2 \hat{\boldsymbol{\Sigma}}_{\mathbf{h}}\right) \tag{A.3}$$

where the covariance matrix $\sigma_\varepsilon^2 \hat{\boldsymbol{\Sigma}}_{\mathbf{h}}$ equals to the inverse of Hessian matrix $\mathbf{H}(\hat{\mathbf{h}},\sigma_\varepsilon)$ of the function $L(\mathbf{h},\sigma_\varepsilon)$ evaluated at $\hat{\mathbf{h}}$ and given by $\frac{n_q}{\sigma_\varepsilon^2}\mathbf{H}(\hat{\mathbf{h}})$, where

$$\mathbf{H}(\hat{\mathbf{h}}) = \left. \frac{\partial^2 J(\mathbf{h};\{y_k\},\{\tilde{q}_k\})}{\partial \mathbf{h}^{\mathrm{T}} \partial \mathbf{h}} \right|_{\mathbf{h}=\hat{\mathbf{h}}} \tag{A.4}$$

So the covariance matrix $\hat{\boldsymbol{\Sigma}}_{\mathbf{h}}$ is given by $\hat{\boldsymbol{\Sigma}}_{\mathbf{h}} = \frac{1}{n_q}\mathbf{H}^{-1}(\hat{\mathbf{h}})$. The MPV can be directly computed using an optimization tool, while the hessian matrix can be computed numerically or analytically [40,41].

Credit Author Statement

Menghao Ping: Conceptualization, Methodology, Formal Analysis, Investigation, Validation, Visualization, Data curation, Software, Writing - Original Draft.
Xinyu Jia: Conceptualization, Methodology, Software, Writing - Original Draft.
Costas Papadimitriou: Conceptualization, Funding Acquisition, Project Administration, Writing - Review & Editing.
Xu Han: Conceptualization, Writing - Review & Editing.
Chao Jiang: Conceptualization, Writing - Review & Editing.

References

[1] Beck J L, Katafygiotis L S. Updating models and their uncertainties. I: Bayesian statistical framework. Journal of Engineering Mechanics, 1998, 124(4): 455-461.
[2] Katafygiotis L S, Papadimitriou C, Lam H F. A probabilistic approach to structural model updating. Soil Dynamics and Earthquake Engineering, 1998, 17(7-8): 495-507.

[3] Vanik M W, Beck J L, Au S K. Bayesian probabilistic approach to structural health monitoring. Journal of Engineering Mechanics, 2000, 126(7): 738-745.
[4] Beck J L, Au S K. Bayesian updating of structural models and reliability using Markov chain Monte Carlo simulation. Journal of engineering mechanics, 2002, 128(4): 380-391.
[5] Johnson E A, Lam H F, Katafygiotis L S, et al. Phase I IASC-ASCE structural health monitoring benchmark problem using simulated data. Journal of engineering mechanics, 2004, 130(1): 3-15.
[6] Beck J L. Bayesian system identification based on probability logic. Structural Control and Health Monitoring, 2010, 17(7): 825-847.
[7] Straub D, Papaioannou I. Bayesian updating with structural reliability methods. Journal of Engineering Mechanics, 2015, 141(3): 04014134.
[8] Beck J L, Yuen K V. Model selection using response measurements: Bayesian probabilistic approach. Journal of Engineering Mechanics, 2004, 130(2): 192-203.
[9] Yuen K V. Bayesian methods for structural dynamics and civil engineering. John Wiley & Sons, 2010.
[10] Sohn H, Law K H. A Bayesian probabilistic approach for structure damage detection. Earthquake engineering & structural dynamics, 1997, 26(12): 1259-1281.
[11] Yuen K V, Beck J L, Au S K. Structural damage detection and assessment by adaptive Markov chain Monte Carlo simulation. Structural Control and Health Monitoring, 2004, 11(4): 327-347.
[12] Yuen K V, Beck J L, Katafygiotis L S. Unified probabilistic approach for model updating and damage detection. 2006.
[13] Papadimitriou C, Beck J L, Katafygiotis L S. Updating robust reliability using structural test data. Probabilistic engineering mechanics, 2001, 16(2): 103-113.
[14] Beck J L, Taflanidis A. Prior and posterior robust stochastic predictions for dynamical systems using probability logic. International Journal for Uncertainty Quantification, 2013, 3(4).
[15] Cornwell P, Farrar C R, Doebling S W, et al. Environmental variability of modal properties. Experimental techniques, 1999, 23(6): 45-48.
[16] Alampalli S. Effects of testing, analysis, damage, and environment on modal parameters. Mechanical Systems and Signal Processing, 2000, 14(1): 63-74.
[17] Moser P, Moaveni B. Environmental effects on the identified natural frequencies of the Dowling Hall Footbridge. Mechanical Systems and Signal Processing, 2011, 25(7): 2336-2357.
[18] Ballesteros G C, Angelikopoulos P, Papadimitriou C, et al. Bayesian hierarchical models for uncertainty quantification in structural dynamics//Vulnerability, uncertainty, and risk: Quantification, mitigation, and management. 2014: 1615-1624.
[19] Nagel J B, Sudret B. A unified framework for multilevel uncertainty quantification in Bayesian inverse problems. Probabilistic Engineering Mechanics, 2016, 43: 68-84.
[20] Rouder J N, Lu J. An introduction to Bayesian hierarchical models with an application in the theory of signal detection. Psychonomic bulletin & review, 2005, 12(4): 573-604.
[21] Behmanesh I, Moaveni B, Lombaert G, et al. Hierarchical Bayesian model updating for structural identification. Mechanical Systems and Signal Processing, 2015, 64: 360-376.
[22] Behmanesh I, Moaveni B. Accounting for environmental variability, modeling errors, and parameter estimation uncertainties in structural identification. Journal of Sound and Vibration, 2016, 374: 92-110.
[23] Wu S, Angelikopoulos P, Beck J L, et al. Hierarchical Stochastic Model in Bayesian Inference for Engineering Applications: Theoretical Implications and Efficient Approximation. ASCE-ASME J Risk and Uncert in Engrg Sys Part B Mech Engrg, 2019, 5(1).
[24] Sedehi O, Papadimitriou C, Katafygiotis L S. Probabilistic hierarchical Bayesian framework for time-domain model updating and robust predictions. Mechanical Systems and

Signal Processing, 2019, 123: 648-673.
[25] Sedehi O, Papadimitriou C, Katafygiotis L S. Data-driven uncertainty quantification and propagation in structural dynamics through a hierarchical Bayesian framework. Probabilistic Engineering Mechanics, 2020, 60: 103047.
[26] Patsialis D, Kyprioti A P, Taflanidis A A. Bayesian calibration of hysteretic reduced order structural models for earthquake engineering applications. Engineering Structures, 2020, 224: 111204.
[27] Jaynes E T. Information theory and statistical mechanics . Physical review, 1957, 106(4): 620.
[28] Sobczyk K, Trcebicki J. Approximate probability distributions for stochastic systems: maximum entropy method . Computer Methods in Applied Mechanics and Engineering, 1999, 168(1-4): 91-111.
[29] Scott D W. Multivariate density estimation: theory, practice, and visualization . John Wiley & Sons, 2015.
[30] Yang C , Duraiswami R , Gumerov N A , et al. Improved Fast Gauss Transform and Efficient Kernel Density Estimation. Null. IEEE Computer Society, 2003.
[31] Kullback S, Leibler R A. On information and sufficiency. The annals of mathematical statistics, 1951, 22(1): 79-86.
[32] Coughlin M, Christensen N, Gair J, et al. Method for estimation of gravitational-wave transient model parameters in frequency–time maps. Classical and Quantum Gravity, 2014, 31(16): 165012.
[33] Rahman S, Xu H. A univariate dimension-reduction method for multi-dimensional integration in random mechanics. Probabilistic Engineering Mechanics, 2004, 19(4):393-408.
[34] Sedehi O, Katafygiotis L S, Papadimitriou C. Hierarchical Bayesian operational modal analysis: Theory and computations. Mechanical Systems and Signal Processing, 2020, 140: 106663.
[35] Basquin O H. The exponential law of endurance tests. Proc Am Soc Test Mater. 1910, 10: 625-630.
[36] Guida M, Penta F. A Bayesian analysis of fatigue data. Structural Safety, 2010, 32(1): 64-76.
[37] Xie L, Liu J, Wu N, et al. Backwards statistical inference method for P–S–N curve fitting with small-sample experiment data. International Journal of Fatigue, 2014, 63: 62-67.
[38] Liu X W, Lu D G, Hoogenboom P C J. Hierarchical Bayesian fatigue data analysis. International Journal of Fatigue, 2017, 100: 418-428.
[39] Chen J, Liu S, Zhang W, et al. Uncertainty quantification of fatigue SN curves with sparse data using hierarchical Bayesian data augmentation. International Journal of Fatigue, 2020, 134: 105511.
[40] H. Jensen, C. Papadimitriou, Bayesian Finite Element Model Updating, in: Sub-Structure Coupling for Dynamic Analysis, Springer, 2019: pp. 179–227. https://doi.org/10.1007/978-3-030-12819-7_7
[41] E. Ntotsios, C. Papadimitriou, Multi-objective optimization algorithms for finite element model updating, in: 23rd International Conference on Noise and Vibration Engineering 2008, ISMA 2008, 2008: pp. 1895–1909. https://repository.lboro.ac.uk/account/articles/9430766.